



This is a repository copy of *Analysis of the fourth-order co-array for a mixture of circular and noncircular signals*.

White Rose Research Online URL for this paper:

<https://eprints.whiterose.ac.uk/194182/>

Version: Accepted Version

---

**Article:**

Cai, J., Li, P., Liu, W. [orcid.org/0000-0003-2968-2888](https://orcid.org/0000-0003-2968-2888) et al. (2 more authors) (2022) Analysis of the fourth-order co-array for a mixture of circular and noncircular signals. Digital Signal Processing. 103857. ISSN 1051-2004

<https://doi.org/10.1016/j.dsp.2022.103857>

---

Article available under the terms of the CC-BY-NC-ND licence (<https://creativecommons.org/licenses/by-nc-nd/4.0/>).

**Reuse**

This article is distributed under the terms of the Creative Commons Attribution-NonCommercial-NoDerivs (CC BY-NC-ND) licence. This licence only allows you to download this work and share it with others as long as you credit the authors, but you can't change the article in any way or use it commercially. More information and the full terms of the licence here: <https://creativecommons.org/licenses/>

**Takedown**

If you consider content in White Rose Research Online to be in breach of UK law, please notify us by emailing [eprints@whiterose.ac.uk](mailto:eprints@whiterose.ac.uk) including the URL of the record and the reason for the withdrawal request.



[eprints@whiterose.ac.uk](mailto:eprints@whiterose.ac.uk)  
<https://eprints.whiterose.ac.uk/>

# Analysis of the Fourth-Order Co-Array for a Mixture of Circular and Noncircular Signals

Jingjing Cai<sup>a,\*</sup>, Panpan Li<sup>a</sup>, Wei Liu<sup>b,\*\*</sup>, Dan Bao<sup>a</sup>, Yangyang Dong<sup>a</sup>

<sup>a</sup>Department of Electronic Engineering, Xidian University, Xi'an, 710071, China

<sup>b</sup>Department of Electronic and Electrical Engineering, University of Sheffield, Sheffield, S1 4ET, United Kingdom

---

## Abstract

A detailed analysis of the degrees of freedom (DOFs) (and therefore the maximum number of signals to be estimated) of the fourth-order sum and difference co-arrays for direction of arrival (DOA) estimation in the presence of circular, strictly noncircular and nonstrictly noncircular signals is presented. There are different ways in combining noncircularity, fourth-order cumulants and sparse arrays to increase the DOFs of the system for DOA estimation. However, there are some confusions or a lack of clarity in the combination. In this work, we aim to fill the gap and clarify some relevant issues by providing a detailed analysis for the fourth-order co-array for a mixture of circular, strictly noncircular and nonstrictly noncircular signals based on a general signal model, including consideration of the noncircular phases of signals in DOA estimation, the fourth-order co-array aperture by considering all the fourth-order cumulants, the difference in the number of signals to be resolved for the strictly and nonstrictly noncircular signals, and the general analysis of DOFs for a mixture of circular, strictly noncircular and nonstrictly noncircular signals based on either uniform or sparse arrays. Furthermore, the expansion and shift scheme with one sub-array being a nested array and another one being a stamp array is proposed, which provides the most DOFs among considered sparse array construction schemes.

*Keywords:* Sparse arrays, fourth-order co-array, sum co-array, difference co-array, noncircularity.

---

## 1. Introduction

For direction of arrival (DOA) estimation, one of the most important problems is how to increase the degrees of freedom (DOFs) of the array for underdetermined estimation. There are three widely adopted approaches: using the noncircular properties of the signals, exploiting higher-order statistics of the signals, in particular the fourth-order cumulants, and employing various sparse array structures. For the first approach, in the presence of noncircular signals, both the covariance and pseudo covariance matrices can be employed to create a much larger virtual array [1, 2, 3, 4, 5]. The fourth-order cumulant based DOA estimation algorithms provide greater DOFs than the second-order based algorithms, and the influence of Gaussian noise can be eliminated at the same time, although at the cost of a very high computational complexity [6, 7, 8, 9]. For sparse arrays, a difference co-array operation is normally performed, generating a significantly larger virtual co-array for underdetermined DOA estimation, and representative examples include co-prime arrays (CPAs) and nested arrays (NAs) [10, 11, 12, 13, 14].

Moreover, two or all three of the approaches can be combined together to increase the DOFs further. Examples include algorithms combining the noncircular properties and the fourth-order cumulants [15, 16, 17, 18, 19], combining the noncircular properties and sparse arrays [20, 21, 22, 23], or combining the

fourth-order cumulants and sparse arrays [24, 25, 26, 27, 28]. In [29], all the three approaches are employed together.

However, there are different ways of combining noncircularity, fourth-order cumulants and sparse arrays together and there are possible confusions or at least a lack of clarity in the combination, as listed below.

1) The noncircular phases of different signals are not considered in the signal model in some existing works. Although this may greatly increase the virtual co-array aperture, it is not realistic in some practical scenarios to assume the noncircular phase information is known [15, 21, 29].

2) The extended covariance matrix used in these works normally ignore the fourth-order cumulants  $\text{cum}[x_i^*(t), x_j^*(t), x_u^*(t), x_v^*(t)]$  (or  $\text{cum}[x_i(t), x_j(t), x_u(t), x_v(t)]$ ), and only focuses on  $\text{cum}[x_i(t), x_j^*(t), x_u(t), x_v^*(t)]$  and  $\text{cum}[x_i^*(t), x_j(t), x_u^*(t), x_v(t)]$  (or  $\text{cum}[x_i^*(t), x_j(t), x_u(t), x_v(t)]$ ), where  $x_l(t)$  is the received signal of the  $l$ -th sensor in an array and the other parameters can be found in Sec. 2. Whether the additional types of fourth-order cumulants can help extend the virtual co-array aperture further or not has not been studied in literature yet [6, 16, 17].

3) The ‘noncircular signal’ mentioned in these works is mainly focused on the ‘strictly noncircular signal’, and the possible impact of the nonstrictly noncircular signals on the maximum number of signals to be estimated is often ignored [5, 6, 16, 17, 18, 21].

4) There is a lack of general analysis of DOFs and the maximum number of resolvable signals by the fourth-order co-array for a mixture of circular, strictly noncircular and nonstrictly noncircular signals based on either uniform or sparse arrays.

---

\*Corresponding author

\*\*Corresponding author

Email addresses: jjcai@mail.xidian.edu.cn (Jingjing Cai), w.liu@sheffield.ac.uk (Wei Liu)

In this work, we aim to fill the gap and clarify some relevant issues by providing a detailed analysis for the fourth-order co-array for a mixture of circular, strictly noncircular and non-strictly noncircular signals based on a general signal model. The following is a list of important findings through our analysis:

1) Considering different noncircular phases of different signals, different types of fourth-order cumulants can not be mixed directly in the extended covariance matrix.

2) The fourth-order cumulant of the array signals  $\text{cum}[x_i^*(t), x_j^*(t), x_u^*(t), x_v^*(t)]$  (or  $\text{cum}[x_i(t), x_j(t), x_u(t), x_v(t)]$ ) does not contribute to the DOFs of the array.

3) Only the strictly noncircular signals contribute to increasing the maximum number of resolvable signals by the fourth-order co-array, while the nonstrictly noncircular signals do not, and they play a similar role as the circular ones.

4) The rank of the extended covariance matrix is calculated as  $(2K - K_{\text{snc}})$ , which determines the number of signals to be resolved by the array as  $(2K - K_{\text{snc}}) \leq (L_d + L_s)/2 - 1$ , where  $K$  and  $K_{\text{snc}}$  are the numbers of total signals and strictly noncircular signals, and  $L_d$  and  $L_s$  are the maximum number of consecutive fourth-order cumulants of  $\text{cum}[x_i(t), x_j^*(t), x_u(t), x_v^*(t)]$  and  $\text{cum}[x_i(t), x_j^*(t), x_u^*(t), x_v^*(t)]$  (or  $\text{cum}[x_i^*(t), x_j(t), x_u(t), x_v(t)]$ ), separately.

To demonstrate the result of the above analysis, an example sparse array using the fourth-order cumulants for a mixture of circular and noncircular signals is presented. The expanding and shift (EAS) scheme is an effective sparse array construction methods using the fourth-order cumulants [25, 26], but it is designed without considering the effect of noncircular cumulants. By considering the noncircularity related fourth-order cumulants, two new sparse arrays called EASNC-NA-STA and EASNC-STA-NA with the first sub-array being a nested array and the second one being a stamp array or vice versa are proposed to further increase the DOFs of the array, where the stamp array is designed for maximising the DOFs of the second-order sum co-array [30, 31, 32, 33]. To exploit the DOFs of the array, a MUSIC-type estimation algorithm is employed.

This paper is organized as follows. The array model, detailed analysis of the fourth-order cumulants and the extended covariance matrix are given in Sec. 2. The EASNC-NA-STA and EASNC-STA-NA schemes based on the fourth-order co-array are presented in Sec. 3. Simulation results are provided in Sec. 4 and conclusions are drawn in Sec. 5.

## 2. The Signal Model and Fourth-order Co-array Analysis

### 2.1. The Signal Model

Suppose there are  $K$  far-field independent non-Gaussian narrowband signals  $s_k(t)$  ( $k = 1, \dots, K$ ) impinging on an  $M$ -sensor sparse linear array (SLA) with angle  $\theta_k$  and power  $\eta_k$ . Among these signals, the first  $K_{\text{nc}}$  signals are noncircular, while the last  $K_{\text{c}}$  are circular, and the first  $K_{\text{snc}}$  signals among the noncircular ones are strictly noncircular. The observed signal  $x_m(t)$  at the

$m$ th sensor is given by

$$x_m(t) = \sum_{k=1}^K \Theta_k^{p_m} s_k(t) + n_m(t), \quad (1)$$

where  $\Theta_k = \exp(-j2\pi d \cos\theta_k/\lambda)$ , the unit spacing  $d$  is equal to half wavelength  $\lambda/2$ ,  $p_m$  represents the position of the  $m$ -th sensor, and  $n_m(t)$  is the additive Gaussian noise of the  $m$ th sensor, which is independent of the signals.

For a mixture of circular and noncircular signals, both the covariance matrix  $\text{E}[x_i(t)x_j^H(t)]$  and the pseudo-covariance matrix  $\text{E}[x_i(t)x_j^T(t)]$  are non-zero valued, where  $\text{E}[\cdot]$  is the mathematical expectation,  $(\cdot)^H$  and  $(\cdot)^T$  denote the conjugate transpose and transpose, separately. Suppose  $1 \leq i, j, u, v \leq M$ ,  $\{i, j, u, v\} \in Z$ , and then all the fourth-order cumulants of the  $i$ th,  $j$ th,  $u$ th and  $v$ th sensor received signals can be defined as [29]

$$\begin{aligned} C(i, -j, u, -v) &= \text{cum}[x_i(t), x_j^*(t), x_u(t), x_v^*(t)] \\ C(-i, j, -u, v) &= C^*(i, -j, u, -v) \\ C(i, -j, -u, -v) &= \text{cum}[x_i(t), x_j^*(t), x_u^*(t), x_v^*(t)] \\ C(-i, j, u, v) &= C^*(i, -j, -u, -v) \\ C(i, j, u, v) &= \text{cum}[x_i(t), x_j(t), x_u(t), x_v(t)] \\ C(-i, -j, -u, -v) &= C^*(i, j, u, v), \end{aligned} \quad (2)$$

with

$$\begin{aligned} \text{cum}[y_1, y_2, y_3, y_4] &= \text{E}[y_1 y_2 y_3 y_4] - \text{E}[y_1 y_2] \text{E}[y_3 y_4] \\ &\quad - \text{E}[y_1 y_3] \text{E}[y_2 y_4] - \text{E}[y_1 y_4] \text{E}[y_2 y_3], \end{aligned} \quad (3)$$

where  $(\cdot)^*$  denotes the complex conjugate operation,  $\text{cum}[\cdot]$  denotes the fourth-order cumulant operation, and  $y_1, y_2, y_3, y_4$  are the four elements in the fourth-order cumulant calculation.

Among these fourth-order cumulants,  $C(i, -j, u, -v)$  only contains  $\text{E}[x_i(t)x_j^H(t)]$ , which is non-zero in all situations.  $C(i, -j, -u, -v)$  and  $C(-i, j, u, v)$  have both  $\text{E}[x_i(t)x_j^H(t)]$  and  $\text{E}[x_i(t)x_j^T(t)]$ , while  $C(-i, -j, -u, -v)$  and  $C(i, j, u, v)$  is only related to  $\text{E}[x_i(t)x_j^T(t)]$ , so they are non-zero when noncircular signals are present. Substituting (1) into the fourth-order cumulants, we have [25]

$$\begin{aligned} C(i, -j, u, -v) &= \sum_{k=1}^K \Theta_k^{(p_i - p_j + p_u - p_v)} \cdot C_d(k) \\ C(i, -j, -u, -v) &= \sum_{k=1}^K \Theta_k^{(p_i - p_j - p_u - p_v)} \cdot C_s(k) \\ C(-i, -j, -u, -v) &= \sum_{k=1}^K \Theta_k^{-(p_i + p_j + p_u + p_v)} \cdot C_{\text{ss}}(k), \end{aligned} \quad (4)$$

with

$$\begin{aligned} C_d(k) &= \text{cum}[s_k(t), s_k^*(t), s_k(t), s_k^*(t)] \\ C_s(k) &= \text{cum}[s_k(t), s_k^*(t), s_k^*(t), s_k(t)] \\ C_{\text{ss}}(k) &= \text{cum}[s_k^*(t), s_k^*(t), s_k(t), s_k(t)]. \end{aligned} \quad (5)$$

It can be seen that the fourth-order co-array cumulants  $C(i, -j, u, -v)$ ,  $C(i, -j, -u, -v)$  and  $C(-i, -j, -u, -v)$  correspond

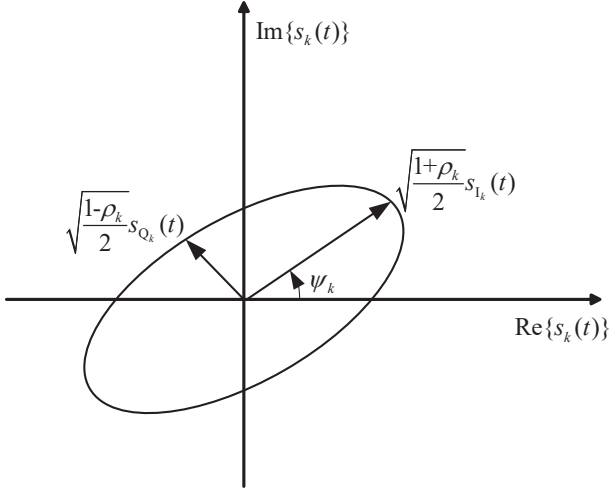


Figure 1: A general complex-valued signal model.

to the virtual array lags  $(p_i - p_j) - (p_v - p_u)$ ,  $(p_i - p_j) - (p_u + p_v)$  and  $-(p_i + p_j) - (p_u + p_v)$ , separately. It is clear that these lags are the differences between two second-order lags, so the virtual steering vectors generated by these fourth-order cumulants are related to both  $\Theta_k^{(p_i - p_j)}$  and  $\Theta_k^{(p_u + p_v)}$ .

## 2.2. The Fourth-Order Cumulants Analysis

For a more detailed analysis of the fourth-order cumulants, we employ a general signal model for  $s_k(t)$  as [34]

$$s_k(t) = \sqrt{\eta_k} e^{j\psi_k} \left[ \sqrt{\frac{1+\rho_k}{2}} s_{I_k}(t) + j \sqrt{\frac{1-\rho_k}{2}} s_{Q_k}(t) \right], \quad (6)$$

where  $s_{I_k}(t)$  and  $s_{Q_k}(t)$  represent the in-phase and quadrature components of a circular signal,  $\psi_k$  is the rotation phase, and  $\rho_k$  ( $0 \leq \rho_k \leq 1$ ) is the noncircularity rate. For circular signals,  $\rho_k = 0$ , and it is  $\rho_k = 1$  and  $0 < \rho_k < 1$  for strictly noncircular and nonstrictly noncircular signals, separately. As shown in Fig. 1, the signal model in (6) describes an ellipse centered at the origin and rotated by  $\psi_k$ , whose axes are parameterized by  $\rho_k$ .

The components  $s_{I_k}(t)$  and  $s_{Q_k}(t)$  are assumed to be uncorrelated, i.e.  $E[s_{I_k}(t)s_{Q_k}(t)] = E[s_{Q_k}(t)s_{I_k}^3(t)] = E[s_{I_k}(t)s_{Q_k}^3(t)] = 0$ . Suppose  $E[s_{I_k}^2(t)] = E[s_{Q_k}^2(t)] = E[s_{I_k}^4(t)] = E[s_{Q_k}^4(t)] = 1$ . The fourth-order cumulants of  $s_k(t)$  can be obtained according to (3) and (5). Detailed calculation is shown in the appendix.

$$\begin{aligned} C_d(k) &= -\eta_k^2(1 + \rho_k^2) \\ C_s(k) &= -2\eta_k^2\rho_k e^{-j2\psi_k} \\ C_{ss}(k) &= -\eta_k^2(1 + \rho_k^2) e^{-j4\psi_k}. \end{aligned} \quad (7)$$

## 2.3. Extended Covariance Matrix Analysis

As  $i, j, u$  and  $v$  take  $M$  different values, there are  $M^4$  possible cumulant values for  $C(i, -j, u, -v)$ ,  $C(i, -j, -u, -v)$  (or

$C(-i, j, u, v)$  and  $C(-i, -j, -u, -v)$  (or  $C(i, j, u, v)$ ), separately. Although these fourth-order cumulants are four dimensional values, they are usually arranged in two-dimensional matrices to make the analysis simple and easier. Convert these four-dimensional values into two-dimensional values  $C_{d1}(h, l)$ ,  $C_{d2}(h, l)$ ,  $C_{s1}(h, l)$ ,  $C_{s2}(h, l)$ ,  $C_{ss1}(h, l)$  and  $C_{ss2}(h, l)$  as

$$\begin{aligned} C_{d1}(M(i-1) + j, M(u-1) + v) &= C(i, -j, u, -v) \\ &= \sum_{k=1}^K \Theta_k^{(p_i - p_j)} C_d(k) \Theta_k^{(p_u - p_v)} \\ C_{d2}(M(i-1) + u, M(j-1) + v) &= C(i, -j, u, -v) \end{aligned} \quad (8)$$

$$= \sum_{k=1}^K \Theta_k^{(p_i + p_u)} C_d(k) \Theta_k^{-(p_j + p_v)}$$

$$C_{s1}(M(i-1) + j, M(u-1) + v) = C(i, -j, -u, -v)$$

$$= \sum_{k=1}^K \Theta_k^{(p_i - p_j)} C_s(k) \Theta_k^{-(p_u + p_v)}$$

$$C_{s2}(M(i-1) + j, M(u-1) + v) = C(-i, j, u, v)$$

$$= \sum_{k=1}^K \Theta_k^{-(p_i - p_j)} C_s^*(k) \Theta_k^{(p_u + p_v)}$$

$$C_{ss1}(M(i-1) + j, M(u-1) + v) = C(-i, -j, -u, -v) \quad (9)$$

$$= \sum_{k=1}^K \Theta_k^{-(p_i + p_j)} C_{ss}(k) \Theta_k^{-(p_u + p_v)}$$

$$C_{ss2}(M(i-1) + j, M(u-1) + v) = C(i, j, u, v)$$

$$= \sum_{k=1}^K \Theta_k^{(p_i + p_j)} C_{ss}^*(k) \Theta_k^{(p_u + p_v)},$$

where  $1 \leq h, l \leq M^2$ . These values can be further arranged in the following form

$$\begin{aligned} C_{d1} &= \mathbf{A}_d \mathbb{R}_d \mathbf{A}_d^H & C_{d2} &= \mathbf{A}_s \mathbb{R}_d \mathbf{A}_s^H \\ C_{s1} &= \mathbf{A}_d \mathbb{R}_s \mathbf{A}_s^H & C_{s2} &= \mathbf{A}_d \mathbb{R}_s^* \mathbf{A}_s^T \\ C_{ss1} &= \mathbf{A}_s^* \mathbb{R}_{ss} \mathbf{A}_s^H & C_{ss2} &= C_{ss1}^* \end{aligned} \quad (10)$$

with

$$\begin{aligned} \mathbb{R}_d &= \text{diag}\{C_d(1), \dots, C_d(K)\} \\ \mathbb{R}_s &= \text{diag}\{C_s(1), \dots, C_s(K)\} \\ \mathbb{R}_{ss} &= \text{diag}\{C_{ss}(1), \dots, C_{ss}(K)\} \\ \mathbf{A}_d &= [\mathbf{a}_d(\theta_1), \dots, \mathbf{a}_d(\theta_K)] \\ \mathbf{A}_s &= [\mathbf{a}_s(\theta_1), \dots, \mathbf{a}_s(\theta_K)] \\ \mathbf{a}_d(\theta_k) &= \mathbf{a}(\theta_k) \otimes \mathbf{a}^*(\theta_k) \\ \mathbf{a}_s(\theta_k) &= \mathbf{a}(\theta_k) \otimes \mathbf{a}(\theta_k) \\ \mathbf{a}(\theta_k) &= [\Theta_k^{p_1}, \Theta_k^{p_2}, \dots, \Theta_k^{p_M}]^T, \end{aligned} \quad (11)$$

where  $\otimes$  is the Kronecker product, and  $\text{diag}\{\cdot\}$  is a diagonal matrix.

Using all of these fourth-order cumulants, the extended fourth-order covariance matrix can be constructed as

$$\mathbf{Q} = \begin{bmatrix} C_{d1} & C_{s2} & C_{s1} \\ C_{s2}^* & C_{d2} & C_{ss1} \\ C_{s1}^* & C_{ss2} & C_{d2} \end{bmatrix} = \mathbf{A} \mathbf{R} \mathbf{A}^H, \quad (12)$$

with

$$\mathbb{R} = \begin{bmatrix} \mathbb{R}_d & \mathbb{R}_s^* & \mathbb{R}_s \\ \mathbb{R}_s & \mathbb{R}_d^* & \mathbb{R}_{ss} \\ \mathbb{R}_s^* & \mathbb{R}_{ss}^* & \mathbb{R}_d \end{bmatrix} \quad (13)$$

$$\mathbb{A} = \begin{bmatrix} \mathbf{A}_d & \mathbf{0}_{M^2 \times K} & \mathbf{0}_{M^2 \times K} \\ \mathbf{0}_{M^2 \times K} & \mathbf{A}_s^* & \mathbf{0}_{M^2 \times K} \\ \mathbf{0}_{M^2 \times K} & \mathbf{0}_{M^2 \times K} & \mathbf{A}_s \end{bmatrix},$$

where  $\mathbf{0}_{l \times h}$  is an  $l \times h$  all-zero matrix.

Now, the dimension of  $\mathbf{Q}$  is  $3M^2 \times 3M^2$ , but there are a lot of repeated entries in it. The real size of  $\mathbf{Q}$  is concerned with the DOFs of the generated fourth-order virtual co-array, and it will be analyzed below according to the parameters  $\psi_k$  and  $\rho_k$  being known or not.

It can be seen that the elements in  $\mathbb{C}_{d1}$ ,  $\mathbb{C}_{s1}$  and  $\mathbb{C}_{ss1}$  are sums of  $-\eta_k^2(1 + \rho_k^2) \cdot \Theta_k^{(p_i - p_j + p_u - p_v)}$ ,  $-2\eta_k^2 \rho_k e^{-j2\psi_k} \cdot \Theta_k^{(p_i - p_j - p_u - p_v)}$  and  $-\eta_k^2(1 + \rho_k^2) e^{-j4\psi_k} \cdot \Theta_k^{-(p_i + p_j + p_u + p_v)}$ , separately. If the parameters  $\psi_k$  and  $\rho_k$  are assumed to be known as  $\hat{\psi}_k$  and  $\hat{\rho}_k$ , the elements in  $\mathbb{C}_{d1}$ ,  $\mathbb{C}_{s1}$  and  $\mathbb{C}_{ss1}$  are only concerned with the unknown parameter  $\Theta_k$ . In the case  $(p_i - p_j + p_u - p_v)$  of the element in  $\mathbb{C}_{d1}$  and  $(p_i - p_j - p_u - p_v)$  of the element in  $\mathbb{C}_{s1}$  are equal, regardless of  $-(1 + \hat{\rho}_k^2)$  and  $-2\hat{\rho}_k e^{-j2\hat{\psi}_k}$ , the elements in  $\mathbb{C}_{d1}$  and  $\mathbb{C}_{s1}$  are the same, which is the sum of  $\eta_k^2 \Theta_k^{(p_i - p_j + p_u - p_v)}$ , and the same applies to the elements in  $\mathbb{C}_{ss1}$ . In another word, the virtual sensors generated by  $\mathbb{C}_{d1}$ ,  $\mathbb{C}_{d2}$ ,  $\mathbb{C}_{s1}$ ,  $\mathbb{C}_{s2}$ ,  $\mathbb{C}_{ss1}$  and  $\mathbb{C}_{ss2}$  can be mixed, and they may fill the holes of the virtual array for each others. In this situation, the total fourth-order co-array virtual sensor positions is a union of the positions generated by  $\mathbb{C}_{d1}$ ,  $\mathbb{C}_{d2}$ ,  $\mathbb{C}_{s1}$ ,  $\mathbb{C}_{s2}$ ,  $\mathbb{C}_{ss1}$  and  $\mathbb{C}_{ss2}$ , which is written as

$$\hat{\mathbb{P}} = \mathbb{P}_d^\pm \cup \mathbb{P}_s^+ \cup \mathbb{P}_s^- \cup \mathbb{P}_{ss}^+ \cup \mathbb{P}_{ss}^-, \quad (14)$$

with

$$\begin{aligned} \mathbb{P}_d^\pm &= \{p_i - p_j + p_u - p_v\} \\ \mathbb{P}_s^+ &= \{-p_i + p_j + p_u + p_v\} \\ \mathbb{P}_s^- &= \{p_i - p_j - p_u - p_v\} \\ \mathbb{P}_{ss}^+ &= \{p_i + p_j + p_u + p_v\} \\ \mathbb{P}_{ss}^- &= \{-p_i - p_j - p_u - p_v\}. \end{aligned} \quad (15)$$

The DOFs of the virtual co-array depends on the maximum consecutive virtual sensor lags of  $\hat{\mathbb{P}}$  [15, 21, 29].

However, in general  $\psi_k$  and  $\rho_k$  are unknown, and then the elements in  $\mathbb{C}_{d1}$  and  $\mathbb{C}_{s1}$  are clearly not equal to each other even if  $(p_i - p_j + p_u - p_v)$  and  $(p_i - p_j - p_u - p_v)$  are equal, and the same applies to the elements in  $\mathbb{C}_{ss1}$ . So, the virtual co-array sensors generated by  $\mathbb{C}_{d1}$  and  $\mathbb{C}_{d2}$  are different from those of  $\mathbb{C}_{s1}$  and  $\mathbb{C}_{s2}$  or  $\mathbb{C}_{ss1}$  and  $\mathbb{C}_{ss2}$ , separately. Thus, three separated sets of virtual sensor positions are generated as

$$\mathbb{P}_1 = \mathbb{P}_d^\pm \quad \mathbb{P}_2 = \mathbb{P}_s^+ \cup \mathbb{P}_s^- \quad \mathbb{P}_3 = \mathbb{P}_{ss}^+ \cup \mathbb{P}_{ss}^-. \quad (16)$$

The DOFs of the virtual co-array depends on the sum of the maximum consecutive virtual sensor lags of  $\mathbb{P}_1$ ,  $\mathbb{P}_2$  and  $\mathbb{P}_3$  [20]. It will be shown later in the next subsection that the elements concerned with  $\mathbb{P}_{ss}^+ \cup \mathbb{P}_{ss}^-$  provide no contribution to the virtual co-array.

In fact, the DOFs of the systems with the parameters  $\psi_k$  and  $\rho_k$  known and unknown are equal for a uniform linear array, but the number of DOFs of the system with parameters known is usually greater than that with parameters unknown in the general case. A sparse array construction scheme for maximizing the part related to the system with parameters known has been proposed in [29]; however, the setting is not valid for the system with parameters unknown in advance, which is normally the case in practice. A sparse array aiming for maximizing the DOFs with parameters unknown will be presented in Sec. 3 of this paper, together with a comparison of the DOFs of these two schemes. As expected, the number of DOFs will be smaller in general when the parameters are unknown due to less information available to the design.

#### 2.4. Rank of the Extended Covariance Matrix

It is difficult to analyze the rank of the fourth-order covariance matrix  $\mathbf{Q}$  directly. According to [4], the rank of the covariance matrix could be obtained by analyzing the covariance matrices of different types of signals contained in  $\mathbf{Q}$  as given below.

Firstly, the signals are mainly divided into three different types: strictly noncircular signals, nonstrictly noncircular signals and circular signals. For different types of signals, the values of the fourth-order cumulants in (7) are different, as shown in the following.

1. Strictly noncircular signals:  $\rho_k = 1$  (such as BPSK (Binary phase shift keying), PAM (Pulse amplitude modulation) and ASK (Amplitude shift keying) signals).

$$\begin{aligned} C_{d\text{-snc}}(k) &= -2\eta_k^2 \\ C_{s\text{-snc}}(k) &= -2\eta_k^2 e^{-j2\psi_k} \\ C_{ss\text{-snc}}(k) &= -2\eta_k^2 e^{-j4\psi_k}, k = 1, \dots, K_{\text{snc}}, \end{aligned}$$

where the subscript ‘‘snc’’ indicates these three quantities are for strictly noncircular signals.

2. Nonstrictly noncircular signals:  $0 < \rho_k < 1$  (such as UQPSK (Unbalanced quaternary phase shift keying) signals).

$$\begin{aligned} C_{d\text{-nc}}(k) &= -\eta_k^2(1 + \rho_k^2) \\ C_{s\text{-nc}}(k) &= -2\eta_k^2 \rho_k e^{-j2\psi_k} \\ C_{ss\text{-nc}}(k) &= -\eta_k^2(1 + \rho_k^2) e^{-j4\psi_k}, k = K_{\text{snc}} + 1, \dots, K_{\text{nc}}, \end{aligned}$$

where the subscript ‘‘nc’’ indicates these are for nonstrictly noncircular signals.

3. Circular signals:  $\rho_k = 0$  (such as QPSK (Quadrature phase shift keying) signals).

$$\begin{aligned} C_{d\text{-c}}(k) &= -\eta_k^2 \\ C_{s\text{-c}}(k) &= 0 \\ C_{ss\text{-c}}(k) &= -\eta_k^2 e^{-j4\psi_k}, k = K_{\text{nc}} + 1, \dots, K, \end{aligned}$$

where the subscript ‘‘c’’ indicates they are for the case with circular signals.

For the steering ‘vector’  $\mathbb{A}$ , it is rewritten into  $\tilde{\mathbb{A}}$  by reordering the elements, so that the elements are grouped according to the types of signals, i.e., strictly noncircular, nonstrictly noncircular and circular signals. Then, the elements of  $\mathbb{R}$  are also reordered correspondingly to construct a new matrix  $\tilde{\mathbb{R}}$ . The newly constructed  $\mathbf{Q}$  is written as

$$\mathbf{Q} = \tilde{\mathbb{A}} \tilde{\mathbb{R}} \tilde{\mathbb{A}}^H = \mathbb{A}_{\text{snc}} \mathbb{R}_{\text{snc}} \mathbb{A}_{\text{snc}}^H + \mathbb{A}_{\text{nc}} \mathbb{R}_{\text{nc}} \mathbb{A}_{\text{nc}}^H + \mathbb{A}_{\text{c}} \mathbb{R}_{\text{c}} \mathbb{A}_{\text{c}}^H, \quad (17)$$

with

$$\begin{aligned} \tilde{\mathbf{A}} &= [\mathbf{A}_{\text{snc}}, \mathbf{A}_{\text{nc}}, \mathbf{A}_{\text{c}}] \\ \mathbf{A}_{\text{snc}} &= \begin{bmatrix} \mathbf{A}_{\text{d-snc}} & \mathbf{0}_{M^2 \times K_{\text{snc}}} & \mathbf{0}_{M^2 \times K_{\text{snc}}} \\ \mathbf{0}_{M^2 \times K_{\text{snc}}} & \mathbf{A}_{\text{s-snc}}^* & \mathbf{0}_{M^2 \times K_{\text{snc}}} \\ \mathbf{0}_{M^2 \times K_{\text{snc}}} & \mathbf{0}_{M^2 \times K_{\text{snc}}} & \mathbf{A}_{\text{s-snc}} \end{bmatrix} \\ \mathbf{A}_{\text{nc}} &= \begin{bmatrix} \mathbf{A}_{\text{d-nc}} & \mathbf{0}_{M^2 \times (K_{\text{nc}} - K_{\text{snc}})} & \mathbf{0}_{M^2 \times (K_{\text{nc}} - K_{\text{snc}})} \\ \mathbf{0}_{M^2 \times (K_{\text{nc}} - K_{\text{snc}})} & \mathbf{A}_{\text{s-nc}}^* & \mathbf{0}_{M^2 \times (K_{\text{nc}} - K_{\text{snc}})} \\ \mathbf{0}_{M^2 \times (K_{\text{nc}} - K_{\text{snc}})} & \mathbf{0}_{M^2 \times (K_{\text{nc}} - K_{\text{snc}})} & \mathbf{A}_{\text{s-nc}} \end{bmatrix} \quad (18) \\ \mathbf{A}_{\text{c}} &= \begin{bmatrix} \mathbf{A}_{\text{d-c}} & \mathbf{0}_{M^2 \times K_{\text{c}}} & \mathbf{0}_{M^2 \times K_{\text{c}}} \\ \mathbf{0}_{M^2 \times K_{\text{c}}} & \mathbf{A}_{\text{s-c}}^* & \mathbf{0}_{M^2 \times K_{\text{c}}} \\ \mathbf{0}_{M^2 \times K_{\text{c}}} & \mathbf{0}_{M^2 \times K_{\text{c}}} & \mathbf{A}_{\text{s-c}} \end{bmatrix} \end{aligned}$$

$$\begin{aligned} \mathbf{A}_{\text{d-snc}} &= [\mathbf{a}_{\text{d}}(\theta_1), \dots, \mathbf{a}_{\text{d}}(\theta_{K_{\text{snc}}})] \\ \mathbf{A}_{\text{d-nc}} &= [\mathbf{a}_{\text{d}}(\theta_{K_{\text{snc}}+1}), \dots, \mathbf{a}_{\text{d}}(\theta_{K_{\text{nc}}})] \\ \mathbf{A}_{\text{d-c}} &= [\mathbf{a}_{\text{d}}(\theta_{K_{\text{nc}}+1}), \dots, \mathbf{a}_{\text{d}}(\theta_K)] \\ \mathbf{A}_{\text{s-snc}} &= [\mathbf{a}_{\text{s}}(\theta_1), \dots, \mathbf{a}_{\text{s}}(\theta_{K_{\text{snc}}})] \\ \mathbf{A}_{\text{s-nc}} &= [\mathbf{a}_{\text{s}}(\theta_{K_{\text{snc}}+1}), \dots, \mathbf{a}_{\text{s}}(\theta_{K_{\text{nc}}})] \\ \mathbf{A}_{\text{s-c}} &= [\mathbf{a}_{\text{s}}(\theta_{K_{\text{nc}}+1}), \dots, \mathbf{a}_{\text{s}}(\theta_K)] \end{aligned} \quad (19)$$

$$\begin{aligned} \tilde{\mathbf{R}} &= \text{diag}\{\mathbb{R}_{\text{snc}}, \mathbb{R}_{\text{nc}}, \mathbb{R}_{\text{c}}\} \\ \mathbb{R}_{\text{snc}} &= \begin{bmatrix} \mathbf{R}_{\text{d-snc}} & \mathbf{R}_{\text{s-snc}}^* & \mathbf{R}_{\text{s-snc}} \\ \mathbf{R}_{\text{s-snc}} & \mathbf{R}_{\text{d-snc}}^* & \mathbf{R}_{\text{ss-snc}} \\ \mathbf{R}_{\text{s-snc}}^* & \mathbf{R}_{\text{ss-snc}}^* & \mathbf{R}_{\text{d-snc}} \end{bmatrix} \\ \mathbb{R}_{\text{nc}} &= \begin{bmatrix} \mathbf{R}_{\text{d-nc}} & \mathbf{R}_{\text{s-nc}}^* & \mathbf{R}_{\text{s-nc}} \\ \mathbf{R}_{\text{s-nc}} & \mathbf{R}_{\text{d-nc}}^* & \mathbf{R}_{\text{ss-nc}} \\ \mathbf{R}_{\text{s-nc}}^* & \mathbf{R}_{\text{ss-nc}}^* & \mathbf{R}_{\text{d-nc}} \end{bmatrix} \quad (20) \\ \mathbb{R}_{\text{c}} &= \begin{bmatrix} \mathbf{R}_{\text{d-c}} & \mathbf{R}_{\text{s-c}}^* & \mathbf{R}_{\text{s-c}} \\ \mathbf{R}_{\text{s-c}} & \mathbf{R}_{\text{d-c}}^* & \mathbf{R}_{\text{ss-c}} \\ \mathbf{R}_{\text{s-c}}^* & \mathbf{R}_{\text{ss-c}}^* & \mathbf{R}_{\text{d-c}} \end{bmatrix} \end{aligned}$$

$$\begin{aligned} \mathbf{R}_{\text{d-snc}} &= \text{diag}\{C_{\text{d-snc}}(1), \dots, C_{\text{d-snc}}(K_{\text{snc}})\} \\ \mathbf{R}_{\text{d-nc}} &= \text{diag}\{C_{\text{d-nc}}(K_{\text{snc}}+1), \dots, C_{\text{d-nc}}(K_{\text{nc}})\} \\ \mathbf{R}_{\text{d-c}} &= \text{diag}\{C_{\text{d-c}}(K_{\text{nc}}+1), \dots, C_{\text{d-c}}(K)\} \\ \mathbf{R}_{\text{s-snc}} &= \text{diag}\{C_{\text{s-snc}}(1), \dots, C_{\text{s-snc}}(K_{\text{snc}})\} \\ \mathbf{R}_{\text{s-nc}} &= \text{diag}\{C_{\text{s-nc}}(K_{\text{snc}}+1), \dots, C_{\text{s-nc}}(K_{\text{nc}})\} \quad (21) \\ \mathbf{R}_{\text{s-c}} &= \text{diag}\{C_{\text{s-c}}(K_{\text{nc}}+1), \dots, C_{\text{s-c}}(K)\} \\ \mathbf{R}_{\text{ss-snc}} &= \text{diag}\{C_{\text{ss-snc}}(1), \dots, C_{\text{ss-snc}}(K_{\text{snc}})\} \\ \mathbf{R}_{\text{ss-nc}} &= \text{diag}\{C_{\text{ss-nc}}(K_{\text{snc}}+1), \dots, C_{\text{ss-nc}}(K_{\text{nc}})\} \\ \mathbf{R}_{\text{ss-c}} &= \text{diag}\{C_{\text{ss-c}}(K_{\text{nc}}+1), \dots, C_{\text{ss-c}}(K)\}. \end{aligned}$$

Note the relationships of  $C_{\text{d}}(k)$ ,  $C_{\text{s}}(k)$  and  $C_{\text{ss}}(k)$  for different types of signals are

$$\begin{aligned} C_{\text{ss-snc}}(k) &= e^{-j2\psi_k} C_{\text{s-snc}}(k) = e^{-j4\psi_k} C_{\text{d-snc}}(k) \\ C_{\text{ss-nc}}(k) &= e^{-j4\psi_k} C_{\text{d-nc}}(k) \\ C_{\text{ss-c}}(k) &= e^{-j4\psi_k} C_{\text{d-c}}(k). \end{aligned} \quad (22)$$

As there are overlapped elements in each of these three covariance matrices  $\mathbf{A}_{\text{snc}} \mathbb{R}_{\text{snc}} \mathbf{A}_{\text{snc}}^{\text{H}}$ ,  $\mathbf{A}_{\text{nc}} \mathbb{R}_{\text{nc}} \mathbf{A}_{\text{nc}}^{\text{H}}$ , and  $\mathbf{A}_{\text{c}} \mathbb{R}_{\text{c}} \mathbf{A}_{\text{c}}^{\text{H}}$ , and the ranks of  $\mathbb{R}_{\text{snc}}$ ,  $\mathbb{R}_{\text{nc}}$  and  $\mathbb{R}_{\text{c}}$  are not clear, the rank of  $\mathbf{Q}$  can not be analyzed here directly. Then, the expression for  $\mathbf{Q}$  can be updated as

$$\mathbf{Q} = \mathbf{A} \mathbf{R} \mathbf{A}^{\text{H}} = \mathbf{A}_{\text{snc}} \mathbf{R}_{\text{snc}} \mathbf{A}_{\text{snc}}^{\text{H}} + \mathbf{A}_{\text{nc}} \mathbf{R}_{\text{nc}} \mathbf{A}_{\text{nc}}^{\text{H}} + \mathbf{A}_{\text{c}} \mathbf{R}_{\text{c}} \mathbf{A}_{\text{c}}^{\text{H}}, \quad (23)$$

with

$$\begin{aligned} \mathbf{A} &= [\mathbf{A}_{\text{snc}}, \mathbf{A}_{\text{nc}}, \mathbf{A}_{\text{c}}] \\ \mathbf{A}_{\text{snc}} &= \begin{bmatrix} \mathbf{A}_{\text{d-snc}} \mathbf{E}_1 \\ \mathbf{A}_{\text{s-snc}}^* \mathbf{E}_1^* \\ \mathbf{A}_{\text{s-snc}} \mathbf{E}_2 \end{bmatrix} \\ \mathbf{A}_{\text{nc}} &= \begin{bmatrix} \mathbf{A}_{\text{d-nc}} & \mathbf{0}_{M^2 \times (K_{\text{nc}} - K_{\text{snc}})} \\ \mathbf{0}_{M^2 \times (K_{\text{nc}} - K_{\text{snc}})} & \mathbf{A}_{\text{s-nc}}^* \\ \mathbf{0}_{M^2 \times (K_{\text{nc}} - K_{\text{snc}})} & \mathbf{A}_{\text{s-nc}} \mathbf{E}_3 \end{bmatrix} \quad (24) \\ \mathbf{A}_{\text{c}} &= \begin{bmatrix} \mathbf{A}_{\text{d-c}} & \mathbf{0}_{M^2 \times K_{\text{c}}} \\ \mathbf{0}_{M^2 \times K_{\text{c}}} & \mathbf{A}_{\text{s-c}}^* \\ \mathbf{0}_{M^2 \times K_{\text{c}}} & \mathbf{A}_{\text{s-c}} \mathbf{E}_4 \end{bmatrix} \end{aligned}$$

$$\begin{aligned} \mathbf{R} &= \text{diag}\{\mathbf{R}_{\text{snc}}, \mathbf{R}_{\text{nc}}, \mathbf{R}_{\text{c}}\} \\ \mathbf{R}_{\text{snc}} &= \mathbf{R}_{\text{d-snc}} \\ \mathbf{R}_{\text{nc}} &= \begin{bmatrix} \mathbf{R}_{\text{d-nc}} & \mathbf{R}_{\text{s-nc}}^* \\ \mathbf{R}_{\text{s-nc}} & \mathbf{R}_{\text{d-nc}}^* \end{bmatrix} \quad (25) \\ \mathbf{R}_{\text{c}} &= \begin{bmatrix} \mathbf{R}_{\text{d-c}} & \mathbf{R}_{\text{s-c}}^* \\ \mathbf{R}_{\text{s-c}} & \mathbf{R}_{\text{d-c}}^* \end{bmatrix} \end{aligned}$$

$$\begin{aligned} \mathbf{E}_1 &= \text{diag}\{e^{j\psi_1}, \dots, e^{j\psi_{K_{\text{snc}}}}\} \\ \mathbf{E}_2 &= \text{diag}\{e^{j3\psi_1}, \dots, e^{j3\psi_{K_{\text{snc}}}}\} \\ \mathbf{E}_3 &= \text{diag}\{e^{j4\psi_{K_{\text{snc}}+1}}, \dots, e^{j4\psi_{K_{\text{nc}}}}\} \\ \mathbf{E}_4 &= \text{diag}\{e^{j4\psi_{K_{\text{nc}}+1}}, \dots, e^{j4\psi_K}\}. \end{aligned} \quad (26)$$

It can be seen that,  $\mathbf{R}_{\text{snc}}$  is only related to  $C_{\text{d}}(k)$ , while  $\mathbf{R}_{\text{nc}}$  and  $\mathbf{R}_{\text{c}}$  are related to  $C_{\text{d}}(k)$  and  $C_{\text{s}}(k)$ . As a result,  $C_{\text{ss}}(k)$  has no additional contribution to the rank of  $\mathbf{R}$  and the DOFs of the virtual co-array. It can be deduced that compared with the cumulants  $C(i, -j, u, -v)$  and  $C(i, -j, -u, -v)$  (or  $C(-i, j, u, v)$ ), the cumulant  $C(-i, -j, -u, -v)$  (or  $C(i, j, u, v)$ ) has no additional contribution to the DOFs of the system.

Moreover, from the above equation, it can be seen that the rank of  $\mathbf{Q}$  equals that of  $\mathbf{R}$ , which is the sum of the ranks of  $\mathbf{R}_{\text{snc}}$ ,  $\mathbf{R}_{\text{nc}}$  and  $\mathbf{R}_{\text{c}}$ . The rank of  $\mathbf{R}_{\text{snc}}$  equals that of  $\mathbf{R}_{\text{d-snc}}$ , which is  $K_{\text{snc}}$ . The ranks of  $\mathbf{R}_{\text{nc}}$  and  $\mathbf{R}_{\text{c}}$  are equal to twice the rank of  $\mathbf{R}_{\text{d-nc}}$  and  $\mathbf{R}_{\text{d-c}}$ , which are  $2(K_{\text{nc}} - K_{\text{snc}})$  and  $2K_{\text{c}}$ , separately. As a result, the rank of  $\mathbf{Q}$  is calculated as

$$\begin{aligned} r(\mathbf{Q}) &= r(\mathbf{R}_{\text{snc}}) + r(\mathbf{R}_{\text{nc}}) + r(\mathbf{R}_{\text{c}}) \\ &= K_{\text{snc}} + 2(K_{\text{nc}} - K_{\text{snc}}) + 2K_{\text{c}} \\ &= 2(K_{\text{nc}} + K_{\text{c}}) - K_{\text{snc}} \\ &= 2K - K_{\text{snc}}, \end{aligned} \quad (27)$$

where  $r(\cdot)$  is the rank of the matrix.

It can be seen that the presence of strictly noncircular signals has reduced the rank of  $\mathbf{Q}$ , which means that the maximum number of signals to be resolved has been increased; on the other hand, the presence of nonstrictly noncircular signals cannot increase the maximum number of signals to be resolved, which has the same effect as the circular ones.

Suppose the maximum number of consecutive fourth-order cumulants of  $C(i, -j, u, -v)$  and  $C(i, -j, -u, -v)$  (or

$C(-i, j, u, v)$  is  $L_d$  and  $L_s$ , separately. It has been analyzed in [20] that the maximum number of signals to be resolved is  $(2K - K_{\text{snc}}) \leq (L_d + L_s)/2 - 1$  using the ULP (Unequal length plus) algorithm or the ECM (Extended covariance matrix) algorithm proposed there.

### 2.5. The MUSIC-type Algorithm for a Mixture of Circular and Noncircular Signals

Taking the MUSIC-type algorithm as an example, the spatial spectrum function can be written as [35]

$$P(\theta) = \frac{1}{\det\{\bar{\mathbf{A}}^H(\theta)\mathbf{U}_n\mathbf{U}_n^H\bar{\mathbf{A}}(\theta)\}}, \quad (28)$$

with

$$\bar{\mathbf{A}}(\theta) = \begin{bmatrix} \mathbf{a}_d(\theta) & \mathbf{0}_{M^2 \times 1} \\ \mathbf{0}_{M^2 \times 1} & \mathbf{a}_s^*(\theta) \\ \mathbf{0}_{M^2 \times 1} & \mathbf{a}_s(\theta) \end{bmatrix}, \quad (29)$$

where  $\det\{\cdot\}$  is the determinant of its matrix,  $\mathbf{U}_n$  is the noise subspace with size  $3M^2 \times [3M^2 - (2K - K_{\text{snc}})]$ . It should be noticed that the maximum number of signals to be resolved is  $(2K - K_{\text{snc}}) \leq L_s - 1$  for this algorithm, which is a little different from that of the ULP and ECM algorithms [22].

### 2.6. Computational Complexity Analysis

Using the steps above, the original EAS scheme is extended to the case for a mixture of circular and noncircular signals, which is named as the EASNC scheme. The computational complexity of the proposed MUSIC-type algorithm for the EASNC scheme can be summarized as follows:

1. Calculate the fourth-order cumulants of the extended covariance matrix  $\mathbf{Q}$ .

The complexity of computing one fourth-order cumulant is  $9S_{\text{np}}$ , where  $S_{\text{np}}$  represents the number of snapshots. As there are  $3M^2 \times 3M^2$  fourth-order elements in  $\mathbf{Q}$ , the total computational complexity is  $O(9S_{\text{np}} \cdot 9M^4)$ .

2. Eigenvalue decomposition of  $\mathbf{Q}$ .

The noise subspace  $\mathbf{U}_n$  is obtained by eigenvalue decomposition of  $\mathbf{Q}$ , which requires computation of  $O((3M^2)^3)$ .

3. Calculate the spatial spectrum function  $P(\theta)$  for angle searching.

With one constant  $\theta$ , the computation is  $O(2 \cdot 3M^2 \cdot [3M^2 - (2K - K_{\text{snc}})])$ . Suppose  $\hat{K}$  is the number of search angles, and then the total complexity is  $O(2 \cdot 3M^2 \cdot [3M^2 - (2K - K_{\text{snc}})] \cdot \hat{K})$ .

In summary, the computational complexity of the MUSIC-type algorithm is  $O(81M^4S_{\text{np}} + 27M^6 + 6M^2[3M^2 - (2K - K_{\text{snc}})]\hat{K})$ . The analysis above are listed in Table 1.

As a comparison, the computational complexity of the MUSIC-type algorithm for the EAS scheme is analyzed, which is also shown in Table 1.

It can be seen that the computational complexity of the EASNC is higher than that of the EAS, but their magnitudes are almost the same. Suppose  $M = 5$ ,  $S_{\text{np}} = 10$ ,  $K = 10$ ,  $K_c = 2$ ,

$K_{\text{nc}} = 8$ ,  $K_{\text{snc}} = 7$  and  $\hat{K} = 180$ , the computational complexity of the EASNC is almost twice that of the EAS, which are 2602125 and 1034000 for EASNC and EAS, separately.

## 3. The EASNC-NA-STA and EASNC-STA-NA Schemes

### 3.1. The EASNC Scheme

The construction of the EASNC scheme is the same as that of the EAS scheme, which contains two sub-arrays that are both sparse arrays. Suppose an  $M_1$ -sensor array and an  $M_2$ -sensor array are in the positions  $P_1 = \{p_1, \dots, p_{M_1}\} \cdot d$  and  $P_2 = \{q_1, \dots, q_{M_2}\} \cdot d$ , separately. Define the number of consecutive second-order difference co-array lags for  $P_1$  and  $P_2$  as  $B_{D1}$  and  $B_{D2}$ , separately. Expand the positions of  $P_2$  to  $P_2\Delta_E$ , where  $\Delta_E = B_{D1}$ . Then, shift  $P_2\Delta_E$  to  $P_2\Delta_E + \Delta_S$ , where  $\Delta_S = p_{M_1} - q_1 \times \Delta_E$ ; this setting makes the first sensor of  $P_2\Delta_E + \Delta_S$  coincide with the last sensor of  $P_1$ , so that the total number of sensors is  $M = M_1 + M_2 - 1$  due to the one shared sensor. Considering  $P_1$  and  $P_2\Delta_E + \Delta_S$  as the first and second sub-arrays of the EASNC scheme, separately, the sensor positions of the final design are given by the following set [25, 26]

$$P = \{p_1, \dots, p_{M_1}, p_{M_1+1}, \dots, p_M\} \cdot d, \quad (30)$$

where  $p_{M_1+(l-1)} = q_l \times \Delta_E + \Delta_S$ ,  $l = 1, \dots, M_2$ .

As mentioned in last section, the maximum number of signals that can be resolved depends on the value  $(L_d + L_s)/2 - 1$ . The value of  $L_d$  related to  $C(i, -j, u, -v)$  has been analyzed in [25], which is  $L_d = B_{D1}B_{D2}$ . Furthermore, if the first sub-array satisfies  $p_{M_1} - p_1 \leq B_{D1} - 1$ , then the consecutive fourth-order lags will be increased to  $L_d = B_{D1}B_{D2} + 2(p_{M_1} - p_1)$ , and this requirement is almost satisfied by all existing sparse arrays [25]. In the EAS scheme, the maximum number of resolvable signals is  $K \leq (L_d - 1)/2$ .

The value of  $L_s$  concerned with  $C(-i, j, u, v)$  (or  $C(i, -j, -u, -v)$ ) has never been considered in a general expression before, and in the following we try to provide an analysis. Define the number of consecutive second-order sum co-array lags for  $P_1$  and  $P_2$  as  $B_{S1}$  and  $B_{S2}$ , separately. The consecutive segment generated by  $(p_j - p_i)$  is from  $(1 - B_{D1})/2$  to  $(B_{D1} - 1)/2$ , with 0 as the center, and there are  $B_{D1}$  elements in it, while  $(p_u + p_v)$  generates a consecutive segment from  $\Delta_b$  to  $\Delta_b + B_{S2} - 1$ , where  $\Delta_b$  is the first consecutive lag. The lag  $(-p_i + p_j + p_u + p_v)$  related to  $C(-i, j, u, v)$  can be written as  $(p_j - p_i) + (p_u + p_v)$ , which can be seen as the consecutive segment generated by  $(p_j - p_i)$  shifted to the consecutive positions generated by  $(p_u + p_v)$ . In order to ensure that there is no overlap or gap between the shifted segments, the expanding value  $\Delta_E$  should be equal to  $B_{D1}$ . It makes the segment with  $B_{D1}$  elements shifted to  $B_{S2}$  positions with no overlap or gap, and  $L_s = B_{D1}B_{S2}$  consecutive lags are generated. With the same solution, if we consider  $(p_j - p_i) + (p_u + p_v)$  as the consecutive segment generated by  $(p_u + p_v)$  shifted to the consecutive positions generated by  $(p_j - p_i)$ ,  $\Delta_E$  should be set to  $B_{S1}$ , and  $L_s = B_{S1}B_{D2}$ . An analysis of the two schemes can be found in the next sub-section and a performance comparison will be provided in the simulation section.

Table 1: Computational complexity comparison

Algorithm	EAS	EASNC
Covariance matrix computation	$9S_{\text{np}} \cdot 4M^4$	$9S_{\text{np}} \cdot 9M^4$
Eigenvalue decomposition	$(2M^2)^3$	$(3M^2)^3$
Spectrum searching	$2 \cdot 2M^2 \cdot [2M^2 - (2K_c + K_{\text{nc}})] \cdot \hat{K}$	$2 \cdot 3M^2 \cdot [3M^2 - (2K - K_{\text{snc}})] \cdot \hat{K}$
Total computational complexity	$36M^4S_{\text{np}} + 8M^6 + 4M^2[2M^2 - (2K_c + K_{\text{nc}})]\hat{K}$	$81M^4S_{\text{np}} + 27M^6 + 6M^2[3M^2 - (2K - K_{\text{snc}})]\hat{K}$

Most existing sparse arrays are designed for the second-order difference co-array, which may have a larger second-order difference co-array, but smaller second-order sum co-array. The sum co-array oriented sparse array is rarely studied and next the postage-stamp problem is introduced for its design.

### 3.2. The EASNC-NA-STA and EASNC-STA-NA Schemes

In the global postage-stamp problem, no more than  $h$  elements are picked from a set of  $z$  positive integers, and the sum of these elements can generate a set of continuous integers  $Y = \{1, 2, \dots, y\}$ . Suppose the set of positive integers are  $\mathfrak{X} = \{re_1 = 1 < re_2 < \dots < re_z\}$ , the postage-stamp solution chooses a suitable series of  $re_i$  from  $\mathfrak{X}$  to produce the greatest value for  $y$ . Specifically, the postage-stamp problem in the case  $h = 2$  is very similar to the problem of the second-order sum co-array construction, which finds the maximum number of consecutive lags ( $p_u + p_v$ ). However, there is a little difference between these two problems: the postage-stamp problem with  $h = 2$  chooses no more than two elements from  $\mathfrak{X}$ , while the second-order sum co-array problem chooses exactly two values. To solve this problem, one more lag 0 is added in the set  $\mathfrak{X}$ , so one nonzero element choosing situation for the postage-stamp problem is equivalent to one nonzero element and one zero element choosing situation for the second-order sum co-array problem. Using the newly constructed set of integers as the positions of the stamp array, they generate the maximum number of continuous second-order sum co-array lags theoretically. It has been analyzed that the number of continuous second-order difference and sum lags are the same as  $B_{\text{D-sta}} = B_{\text{S-sta}} = y + 1$  for the stamp array [31, 32].

The number of lags with different number of physical sensors is given in Table 2, and as a comparison, the number of lags for the nested array is given in Table 3, where the sub-array sensor settings are all for their own best performance.

It can be seen from Tables 2 and 3 that  $B_{\text{D-na}} > B_{\text{D-sta}}$  and  $B_{\text{S-sta}} > B_{\text{S-na}}$ . For the two types of EASNC schemes proposed in the last section, the first type with  $L_s = B_{\text{D1}}B_{\text{S2}}$  is preferred with the first sub-array being a nested array and the second one a stamp array, while for the second type with  $L_s = B_{\text{S1}}B_{\text{D2}}$ , it is the other way around. Define the EASNC scheme with the first and second sub-arrays being a nested array and a stamp array

Table 2: The stamp array

Number of sensors	Array setting	$B_{\text{D-sta}}, B_{\text{S-sta}}$
3	0 1 2	5
4	0 1 3 4	9
5	0 1 3 5 6	13
6	0 1 3 5 7 8	17
7	0 1 2 5 8 9 10	21
8	0 1 2 5 8 11 12 13	27
9	0 1 2 5 8 11 14 15 16	33
10	0 1 3 4 9 11 16 17 19 20	41
11	0 1 2 3 7 11 15 19 21 22 23	47
12	0 1 3 5 6 13 14 21 22 24 26 27	55
13	0 1 3 4 9 11 16 21 23 28 29 31 32	65
14	0 1 3 4 9 11 16 20 25 27 32 33 35 36	73
15	0 1 3 4 5 8 14 20 26 32 35 36 37 39 40	81

Table 3: The nested array

Number of sensors	Array setting	$B_{\text{D-na}}$	$B_{\text{S-na}}$
3	1 2 4	7	5
4	1 2 3 6	11	8
5	1 2 3 6 9	17	11
6	1 2 3 4 8 12	23	15
7	1 2 3 4 8 12 16	31	19
8	1 2 3 4 5 10 15 20	39	24
9	1 2 3 4 5 10 15 20 25	49	29
10	1 2 3 4 5 6 12 18 24 30	59	35
11	1 2 3 4 5 6 12 18 24 30 36	71	41
12	1 2 3 4 5 6 7 14 21 28 35 42	83	49
13	1 2 3 4 5 6 7 14 21 28 35 42 49	97	55
14	1 2 3 4 5 6 7 8 16 24 32 40 48 56	111	63
15	1 2 3 4 5 6 7 8 16 24 32 40 48 56 64	127	71

as EASNC-NA-STA. In the same way, the array EASNC-STA-NA can be defined. Assume the number of sub-array sensors is  $M_1 = M_2 = 5$ , the array setting, the relevant  $L_d$ ,  $L_s$  and the number of signals that can be resolved by the MUSIC-type algorithm are presented in the first two rows in Table 4. It can

be seen that, these two types of algorithms can resolve the same number of signals, which is  $B_{D-na}B_{S-sta} - 1 = 220$ .

Some other schemes EASNC-NA-NA, EAS-NA-NA and EAS-NA-STA are also considered to compare with the proposed EASNC-NA-STA and EASNC-STA-NA schemes. With the setting  $M_1 = M_2 = 5$ , the analysis of these three comparable schemes are shown in the last three rows in Table 4. The maximum number of resolvable signals by the MUSIC-type algorithm is  $B_{D-na}B_{S-na} - 1 = 186$  for the EASNC-NA-NA scheme, and  $(B_{D-na}B_{D-na} + 2(p_{M_1} - p_1) - 1)/2 = 152$ ,  $(B_{D-na}B_{D-sta} + 2(p_{M_1} - p_1) - 1)/2 = 118$  for the EAS-NA-NA and EAS-NA-STA schemes, separately. It is clear that the EASNC-NA-STA and EASNC-STA-NA resolve a greater number of signals than these three schemes.

Now we compare DOFs of the EASNC-NA-STA and EASNC-STA-NA schemes with the scheme proposed in [29], which is based on a known  $\psi_k$ . As an example, the sparse array in [29] generates 219 DOFs with 6 physical sensors, but it requires 9 physical sensors for the EASNC-NA-STA or EASNC-STA-NA schemes to achieve this level of DOFs. As mentioned earlier, this is not surprising, since with known  $\psi_k$  more information is available, which can then be exploited to further increase the DOFs of the system. However, in practice, for most of the cases,  $\psi_k$  will not be available and therefore the presented design of EASNC-NA-STA and EASNC-STA-NA will have more of a practical value.

#### 4. Simulation Results

In this section, simulation results based on the EASNC-NA-STA, EASNC-STA-NA, EASNC-NA-NA, EAS-NA-NA and EAS-NA-STA schemes are provided. The MUSIC-type algorithm is employed to estimate the DOAs, and the full angle range is set from  $-90^\circ$  to  $90^\circ$  with a step size of  $0.1^\circ$ . The total number of physical sensors is  $M = 6$ , the number of sub-array sensors is  $M_1 = 3$  and  $M_2 = 4$  for EASNC-NA-STA, EASNC-NA-NA, EAS-NA-NA and EAS-NA-STA, while it is  $M_1 = 4$  and  $M_2 = 3$  for EASNC-STA-NA. The array setting is  $\{1, 2, 4, 11, 25, 32\} \cdot d$  for EASNC-NA-STA and EAS-NA-STA, and it is  $\{0, 1, 3, 4, 13, 31\} \cdot d$  for EASNC-STA-NA. The number of consecutive fourth-order lags is  $L_d = 69$  and  $L_s = 63$  for EASNC-NA-STA and EAS-NA-STA, and it is  $L_d = 71$  and  $L_s = 63$  for EASNC-STA-NA, separately. So the maximum number of resolvable signals is 62 for EASNC-NA-STA and EASNC-STA-NA, and it is 34 for EAS-NA-STA, respectively. For EASNC-NA-NA and EAS-NA-NA, the array setting is  $\{1, 2, 4, 11, 18, 39\} \cdot d$  with  $L_d = 83$  and  $L_s = 56$ , and then they can resolve at most 55 and 41 signals, respectively. The number of source signals is set to  $K = 13$  and the DOAs are set as  $[-60^\circ, -50^\circ, -40^\circ, -30^\circ, -20^\circ, -10^\circ, 0^\circ, 10^\circ, 20^\circ, 30^\circ, 40^\circ, 50^\circ, 60^\circ]$ . All the noncircular signals are with random initial phases  $\psi_k$ . The number of Monte Carlo trials is 1000 for the last two simulations.

In the first simulation, the signals are set as a mixture of strictly noncircular, non-strictly noncircular and circular signals, where the first 11 DOAs correspond to BPSK signals, the 12th DOA corresponds to a UQPSK signal, and the last one

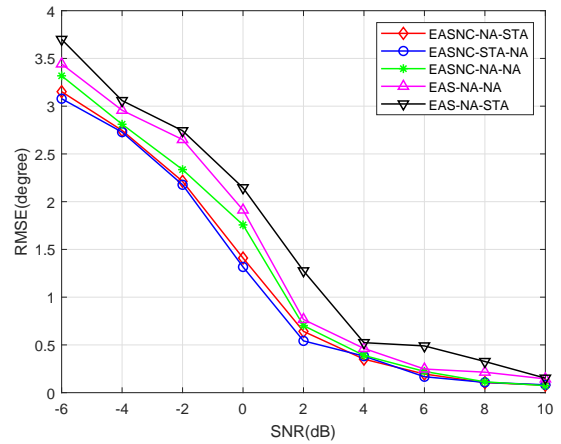


Figure 3: RMSE results with a varied SNR for the mixture of strictly noncircular, nonstrictly noncircular and circular signals.

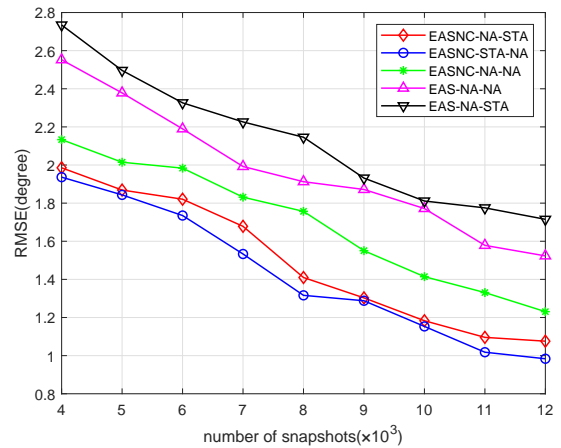


Figure 4: RMSE results with a varied number of snapshots for the mixture of strictly noncircular, nonstrictly noncircular and circular signals.

corresponds to a circular signal. The spatial spectrum results of the four algorithms are shown in Fig. 2. The SNR is set as 0dB and the number of snapshots is 8000. From the figure, we can see that only the EASNC-NA-STA and EASNC-STA-NA schemes have successfully identified all the DOAs, while all the other three have wrong results. Except for EASNC-NA-STA and EASNC-STA-NA, EASNC-NA-NA performs better than the other two, and EAS-NA-STA is the worst.

In the second simulation, the signals are the same set as in the first simulation. The RMSE results versus SNRs are shown in Fig. 3, where the number of snapshots is set as 8000 and the SNR varies from  $-6$ dB to  $10$ dB with a  $2$ dB interval. The RMSE results versus the number of snapshots are shown in Fig. 4, where the SNR is fixed as  $0$ dB and the number of snapshots varies from  $4000$  to  $12000$  with an interval of  $1000$ .

In the third simulation, the signals are set as a mixture of strictly noncircular and circular signals, where the first 11 DOAs correspond to BPSK signals and the last 2 DOAs correspond to circular signals. In the fourth simulation, the signals

Table 4: Analysis of different schemes with  $M_1 = M_2 = 5$ 

Schemes	Array setting	$L_d$	$L_s$	The number of resolved signals
EASNC-NA-STA	1 2 3 6 9 26 60 94 111	237	221	220
EASNC-STA-NA	0 1 3 5 6 19 32 71 110	233	221	220
EASNC-NA-NA	1 2 3 6 9 26 43 94 145	305	187	186
EAS-NA-NA	1 2 3 6 9 26 43 94 145	305		152
EAS-NA-STA	1 2 3 6 9 26 60 94 111	237		118

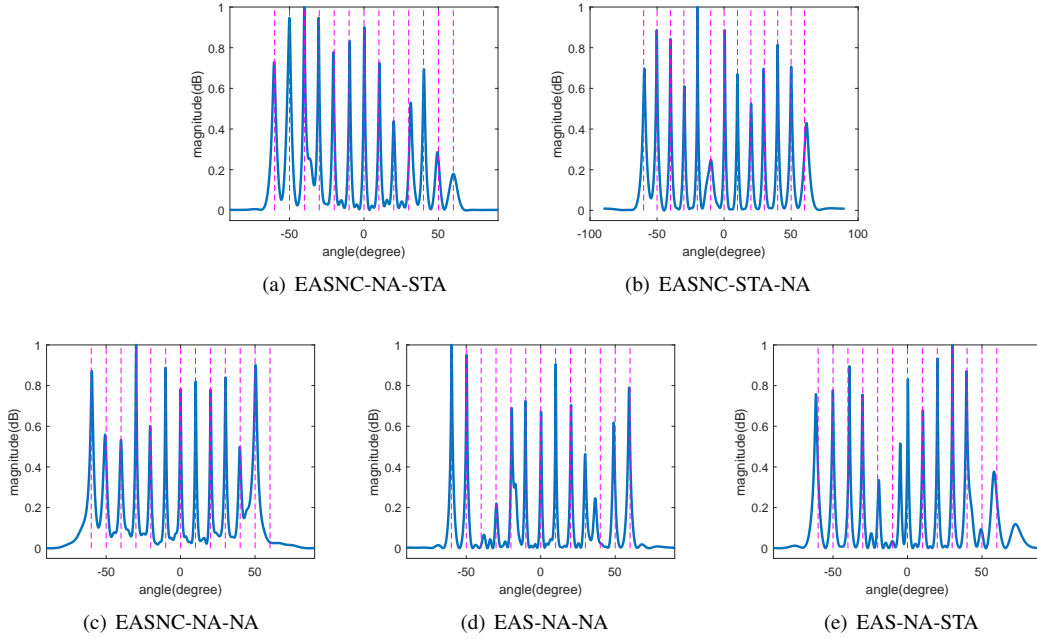


Figure 2: DOA estimation results of the five schemes.

are set as a mixture of strictly noncircular and nonstrictly noncircular signals, where the first 11 DOAs correspond to BPSK signals and the last 2 DOAs correspond to UQPSK signals. The set of the SNRs and the number of snapshots are all the same as those in the second simulation. The DOA estimation results versus SNR are shown in Figs. 5 and 7, while the results versus the number of snapshots are shown in Figs. 6 and 8, separately.

From the figures above, it can be seen that the performance of EASNC-NA-STA and EASNC-STA-NA are almost the same, which are superior to the other three schemes for all mixtures of signals. The EAS-NA-STA and EAS-NA-NA schemes are the worst and second worst of all the schemes, while the EASNC-NA-NA scheme is the third worst one. It can be seen that the EAS schemes without considering the fourth-order cumulants  $C(i, -j, -u, -v)$  and  $C(-i, j, u, v)$  perform worse than the EASNC schemes that consider these cumulants. The EASNC schemes with one nested array and one stamp array as two sub-arrays performs better than that with two nested arrays. Almost in all kinds of SNR and number of snapshots settings, the RMSEs of the EASNC schemes with nested and stamp arrays are  $0.1^\circ$  to  $0.2^\circ$  lower than that with two nested arrays.

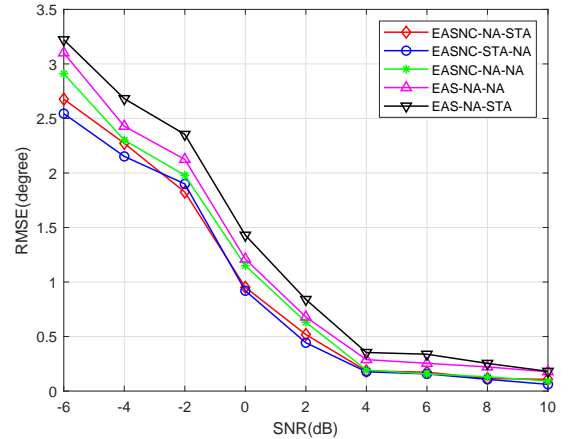


Figure 5: RMSE results with a varied SNR for the mixture of strictly noncircular and circular signals.

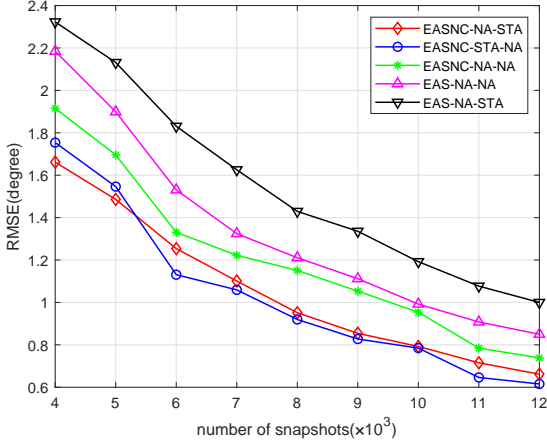


Figure 6: RMSE results with a varied number of snapshots for the mixture of strictly noncircular and circular signals.

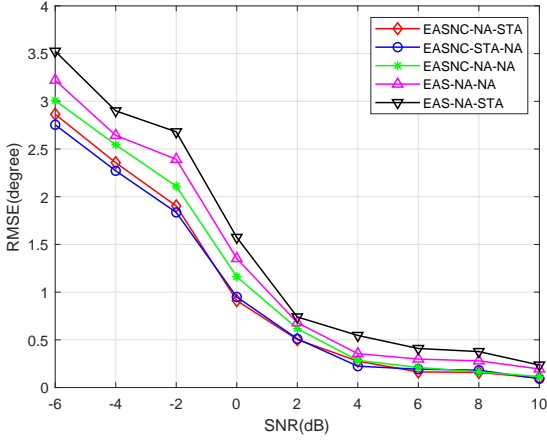


Figure 7: RMSE results with a varied SNR for the mixture of strictly noncircular and nonstrictly noncircular signals.

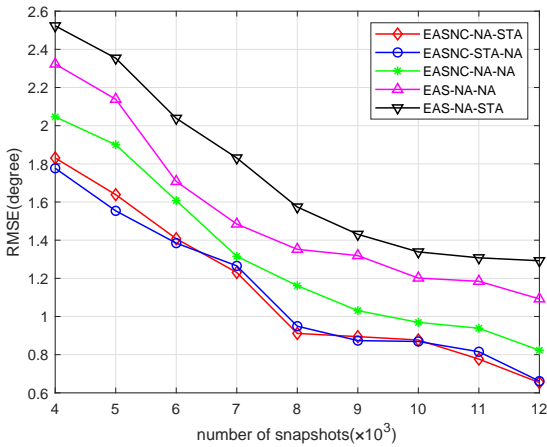


Figure 8: RMSE results with a varied number of snapshots for the mixture of strictly noncircular and nonstrictly noncircular signals.

## 5. Conclusion

An analysis of the DOFs of the fourth-order sum and difference co-array for a mixture of circular, strictly noncircular and nonstrictly noncircular signals has been presented in this paper. Four important conclusions are drawn as stated in the introduction part and the maximum number of resolvable signals by the fourth-order co-array is given as  $(2K - K_{\text{snc}}) \leq (L_d + L_s)/2 - 1$ . The EASNC-NA-STA and EASNC-STA-NA schemes, which are extensions of a previously proposed scheme, but with one sub-array being a nested array and another one being a stamp array, are analyzed as an example, which can resolve a greater number of signals than the other constructions of the EAS-NC or EAS schemes. As demonstrated by simulation results, both EASNC-NA-STA and EASNC-STA-NA have achieved a much better performance than EASNC-NA-NA, EAS-NA-NA and EAS-NA-STA.

## Appendix A.

Substitute the source signal model  $s_k(t)$  into the fourth-order cumulants, and note that  $E[s_{I_k}(t)s_{Q_k}(t)] = E[s_{Q_k}(t)s_{I_k}^3(t)] = E[s_{I_k}(t)s_{Q_k}^3(t)] = 0$ . The cumulant  $\text{cum}[s_k(t), s_k^*(t), s_k(t), s_k^*(t)]$  can be derived as

$$\begin{aligned} & \text{cum}[s_k(t), s_k^*(t), s_k(t), s_k^*(t)] \\ &= E[s_k(t)s_k^*(t)s_k(t)s_k^*(t)] - 2E[s_k(t)s_k^*(t)]E[s_k(t)s_k^*(t)] \\ & \quad - E[s_k(t)s_k(t)]E[s_k^*(t)s_k^*(t)] \\ &= \eta_k^2 \left\{ \left(\frac{1+\rho_k}{2}\right)^2 E[s_{I_k}^4(t)] + \left(\frac{1-\rho_k}{2}\right)^2 E[s_{Q_k}^4(t)] \right. \\ & \quad - 3\left(\frac{1+\rho_k}{2}\right)^2 E[s_{I_k}^2(t)]E[s_{I_k}^2(t)] \\ & \quad \left. - 3\left(\frac{1-\rho_k}{2}\right)^2 E[s_{Q_k}^2(t)]E[s_{Q_k}^2(t)] \right\}, \end{aligned} \quad (\text{A.1})$$

with

$$\begin{aligned} & E[s_k(t)s_k^*(t)s_k(t)s_k^*(t)] \\ &= \eta_k^2 \left\{ \left(\frac{1+\rho_k}{2}\right)^2 E[s_{I_k}^4(t)] + \left(\frac{1-\rho_k}{2}\right)^2 E[s_{Q_k}^4(t)] \right. \\ & \quad \left. + \left(\frac{1-\rho_k^2}{2}\right) E[s_{I_k}^2(t)s_{Q_k}^2(t)] \right\} \\ & E[s_k(t)s_k^*(t)]E[s_k(t)s_k^*(t)] \\ &= \eta_k^2 \left\{ \left(\frac{1+\rho_k}{2}\right)^2 E[s_{I_k}^2(t)]E[s_{I_k}^2(t)] + \left(\frac{1-\rho_k}{2}\right)^2 E[s_{Q_k}^2(t)]E[s_{Q_k}^2(t)] \right. \\ & \quad \left. + \left(\frac{1-\rho_k^2}{2}\right) E[s_{I_k}^2(t)]E[s_{Q_k}^2(t)] \right\} \\ & E[s_k(t)s_k(t)]E[s_k^*(t)s_k^*(t)] \\ &= \eta_k^2 \left\{ \left(\frac{1+\rho_k}{2}\right)^2 E[s_{I_k}^2(t)]E[s_{I_k}^2(t)] + \left(\frac{1-\rho_k}{2}\right)^2 E[s_{Q_k}^2(t)]E[s_{Q_k}^2(t)] \right. \\ & \quad \left. - \left(\frac{1-\rho_k^2}{2}\right) E[s_{I_k}^2(t)]E[s_{Q_k}^2(t)] \right\}. \end{aligned} \quad (\text{A.2})$$

The cumulant  $\text{cum}[s_k(t), s_k^*(t), s_k^*(t), s_k^*(t)]$  is deduced as

$$\begin{aligned} & \text{cum}[s_k(t), s_k^*(t), s_k^*(t), s_k^*(t)] \\ &= \text{E}[s_k(t)s_k^*(t)s_k^*(t)s_k^*(t)] - 3\text{E}[s_k(t)s_k^*(t)]\text{E}[s_k^*(t)s_k^*(t)] \\ &= \eta_k^2 e^{-j2\psi_k} \left\{ \left(\frac{1+\rho_k}{2}\right)^2 \text{E}[s_{I_k}^4(t)] \right. \\ & \quad - \left(\frac{1-\rho_k}{2}\right)^2 \text{E}[s_{Q_k}^4(t)] - 3\left(\frac{1+\rho_k}{2}\right)^2 \text{E}[s_{I_k}^2(t)]\text{E}[s_{I_k}^2(t)] \\ & \quad \left. + 3\left(\frac{1-\rho_k}{2}\right)^2 \text{E}[s_{Q_k}^2(t)]\text{E}[s_{Q_k}^2(t)] \right\}, \end{aligned} \quad (\text{A.3})$$

with

$$\begin{aligned} & \text{E}[s_k(t)s_k^*(t)s_k^*(t)s_k^*(t)] \\ &= \eta_k^2 e^{-j2\psi_k} \left\{ \left(\frac{1+\rho_k}{2}\right)^2 \text{E}[s_{I_k}^4(t)] - \left(\frac{1-\rho_k}{2}\right)^2 \text{E}[s_{Q_k}^4(t)] \right\} \\ & \quad \text{E}[s_k(t)s_k^*(t)]\text{E}[s_k^*(t)s_k^*(t)] \\ &= \eta_k^2 e^{-j2\psi_k} \left\{ \left(\frac{1+\rho_k}{2}\right)^2 \text{E}[s_{I_k}^2(t)]\text{E}[s_{I_k}^2(t)] \right. \\ & \quad \left. - \left(\frac{1-\rho_k}{2}\right)^2 \text{E}[s_{Q_k}^2(t)]\text{E}[s_{Q_k}^2(t)] \right\}. \end{aligned} \quad (\text{A.4})$$

Similarly, the cumulant  $\text{cum}[s_k^*(t), s_k^*(t), s_k^*(t), s_k^*(t)]$  is given by

$$\begin{aligned} & \text{cum}[s_k^*(t), s_k^*(t), s_k^*(t), s_k^*(t)] \\ &= \text{E}[s_k^*(t)s_k^*(t)s_k^*(t)s_k^*(t)] - 3\text{E}[s_k^*(t)s_k^*(t)]\text{E}[s_k^*(t)s_k^*(t)] \\ &= \eta_k^2 e^{-j4\psi_k} \left\{ \left(\frac{1+\rho_k}{2}\right)^2 \text{E}[s_{I_k}^4(t)] + \left(\frac{1-\rho_k}{2}\right)^2 \text{E}[s_{Q_k}^4(t)] \right. \\ & \quad - 3\left(\frac{1+\rho_k}{2}\right)^2 \text{E}[s_{I_k}^2(t)]\text{E}[s_{I_k}^2(t)] \\ & \quad \left. - 3\left(\frac{1-\rho_k}{2}\right)^2 \text{E}[s_{Q_k}^2(t)]\text{E}[s_{Q_k}^2(t)] \right\}, \end{aligned} \quad (\text{A.5})$$

with

$$\begin{aligned} & \text{E}[s_k^*(t)s_k^*(t)s_k^*(t)s_k^*(t)] \\ &= \eta_k^2 e^{-j4\psi_k} \left\{ \left(\frac{1+\rho_k}{2}\right)^2 \text{E}[s_{I_k}^4(t)] + \left(\frac{1-\rho_k}{2}\right)^2 \text{E}[s_{Q_k}^4(t)] \right. \\ & \quad \left. - 3\left(\frac{1-\rho_k^2}{2}\right) \text{E}[s_{I_k}^2(t)s_{Q_k}^2(t)] \right\} \\ & \quad \text{E}[s_k^*(t)s_k^*(t)]\text{E}[s_k^*(t)s_k^*(t)] \\ &= \eta_k^2 e^{-j4\psi_k} \left\{ \left(\frac{1+\rho_k}{2}\right)^2 \text{E}[s_{I_k}^2(t)]\text{E}[s_{I_k}^2(t)] \right. \\ & \quad \left. + \left(\frac{1-\rho_k}{2}\right)^2 \text{E}[s_{Q_k}^2(t)]\text{E}[s_{Q_k}^2(t)] \right. \\ & \quad \left. - \frac{1-\rho_k^2}{2} \text{E}[s_{I_k}^2(t)]\text{E}[s_{Q_k}^2(t)] \right\}. \end{aligned} \quad (\text{A.6})$$

Then, substituting  $\text{E}[s_{I_k}^2(t)] = \text{E}[s_{Q_k}^2(t)] = \text{E}[s_{I_k}^4(t)] = \text{E}[s_{Q_k}^4(t)] = 1$  into these expressions, we can finally obtain

$$\begin{aligned} & \text{cum}[s_k(t), s_k^*(t), s_k(t), s_k^*(t)] = -\eta_k^2(1+\rho_k^2) \\ & \text{cum}[s_k(t), s_k^*(t), s_k^*(t), s_k^*(t)] = -2\eta_k^2\rho_k e^{-j2\psi_k} \\ & \text{cum}[s_k^*(t), s_k^*(t), s_k^*(t), s_k^*(t)] = -\eta_k^2(1+\rho_k^2)e^{-j4\psi_k}. \end{aligned} \quad (\text{A.7})$$

## Acknowledgement

This work was partially supported by the National Natural Science Foundation of China (61805189 and 61901332), the Fundamental Research Funds for the Central Universities (No.JB210201) and the Natural Science Basic Research Plan in Shaanxi Provincial of China (No.2018JQ6068).

## References

- [1] H. Abeida, J. P. Delmas, MUSIC-like estimation of direction of arrival for noncircular sources, *IEEE Transactions on Signal Processing* 54 (7) (2006) 2678–2690.
- [2] H. Chen, C. Hou, W. Liu, W. P. Zhu, M. Swamy, Efficient two-dimensional direction-of-arrival estimation for a mixture of circular and noncircular sources, *IEEE Sensors Journal* 16 (8) (2016) 2527–2536.
- [3] Q. Wang, W. Xian, H. Chen, DOA estimation algorithm for strictly non-circular sources with unknown mutual coupling, *IEEE Communications Letters* 23 (12) (2019) 2215–2218.
- [4] F. Gao, A. Nallanathan, Y. Wang, Improved MUSIC under the coexistence of both circular and noncircular sources, *IEEE Transactions on Signal Processing* 56 (7) (2008) 3033–3038.
- [5] S. Luan, J. Li, Y. Gao, J. Zhang, T. Qiu, Generalized covariance-based ESPRIT-like solution to direction of arrival estimation for strictly non-circular signals under Alpha-stable distributed noise, *Digital Signal Processing* 118 (2021) 103214.
- [6] J. Liu, Z. Huang, Y. Zhou, A direction finding algorithm for noncircular signals based on higher-order cumulants, in: 2007 International Conference on Wireless Communications, Networking and Mobile Computing, 2007, pp. 1044–1047.
- [7] J. F. Cardoso, E. Moulines, Asymptotic performance analysis of direction-finding algorithms based on fourth-order cumulants, *IEEE Transactions on Signal Processing* 43 (1) (1995) 214–224.
- [8] P. Chevalier, L. Albera, A. Ferreol, P. Comon, On the virtual array concept for higher order array processing, *IEEE Transactions on Signal Processing* 53 (4) (2005) 1254–1271.
- [9] U. Sharma, M. Agrawal, 2qth-order cumulants based virtual array of a single acoustic vector sensor, *Digital Signal Processing* (2022) 103438.
- [10] P. Pal, P. Vaidyanathan, Coprime sampling and the MUSIC algorithm, in: *Digital Signal Processing Workshop and IEEE Signal Processing Education Workshop (DSP/SPE)*, 2011, pp. 289–294.
- [11] P. P. Vaidyanathan, P. Pal, Sparse sensing with co-prime samplers and arrays, *IEEE Transactions on Signal Processing* 59 (2) (2011) 573–586.
- [12] P. Pal, P. P. Vaidyanathan, Nested arrays: A novel approach to array processing with enhanced degrees of freedom, *IEEE Transactions on Signal Processing* 58 (8) (2010) 4167–4181.
- [13] A. Raza, W. Liu, Q. Shen, Thinned coprime array for second-order difference co-array generation with reduced mutual coupling, *IEEE Transactions on Signal Processing* 67 (8) (2019) 2052–2065.
- [14] A. H. Shaikh, X. Dang, D. Huang, A pentad-displaced ULAs configuration with hole-free co-array and increased degrees of freedom for direction of arrival estimation, *Digital Signal Processing* 118 (2021) 103243.
- [15] P. Gupta, M. Agrawal, Improved resolving capabilities of linear array using 2qth order noncircular statistics, *IET Signal Processing* 15 (2) (2021) 61–79.
- [16] J. Deng, Q. Wang, J. Xie, Fourth-order cumulant based direction finding algorithm for non-circular signals using uniform circular array with mutual coupling, in: 2020 IEEE International Conference on Signal Processing, Communications and Computing (ICSPCC), 2020, pp. 1–5.
- [17] B. Wang, J. Zheng, Cumulant-based DOA estimation of noncircular signals against unknown mutual coupling, *Sensors* 20 (3) (2020) 878.
- [18] X. Li, Q. Gong, S. Zhong, S. Ren, Near-field noncircular sources localization based on fourth-order cumulant, *IEEE Access* 8 (2020) 120575–120585.
- [19] Y. Yue, Y. Xu, Z. Liu, Root high-order cumulant MUSIC, *Digital Signal Processing* 122 (2022) 103328.
- [20] J. J. Cai, W. Liu, R. Zong, B. Wu, Sparse array extension for non-circular signals with subspace and compressive sensing based DOA estimation methods, *Signal Processing* 145 (2018) 59–67.

- [21] P. Gupta, M. Agrawal, Design and analysis of the sparse array for DOA estimation of noncircular signals, *IEEE Transactions on Signal Processing* 67 (2) (2019) 460–473.
- [22] J. Cai, W. Liu, R. Zong, Y. Dong, A MUSIC-type DOA estimation method based on sparse arrays for a mixture of circular and non-circular signals, in: 2020 IEEE International Conference on Signal Processing, Communications and Computing (ICSPCC), 2020, pp. 1–5.
- [23] J. Zhang, T. Qiu, S. Luan, H. Li, Bounded non-linear covariance based ESPRIT method for noncircular signals in presence of impulsive noise, *Digital Signal Processing* 87 (2019) 104–111.
- [24] P. Chevalier, A. Ferreol, On the virtual array concept for the fourth-order direction finding problem, *IEEE Transactions on Signal Processing* 47 (9) (1999) 2592–2595.
- [25] J. J. Cai, W. Liu, R. Zong, Q. Shen, An expanding and shift scheme for constructing fourth-order difference co-arrays, *IEEE Signal Processing Letters* 24 (4) (2017) 480–484.
- [26] J. J. Cai, W. Liu, R. Zong, B. Wu, An improved expanding and shift scheme for the construction of fourth-order difference co-arrays, *Signal Processing* 153 (2018) 95–100.
- [27] Q. Shen, W. Liu, W. Cui, S. L. Wu, Extension of co-prime arrays based on the fourth-order difference co-array concept, *IEEE Signal Processing Letters* 23 (5) (2016) 615–619.
- [28] Q. Shen, W. Liu, W. Cui, S. Wu, Extension of nested arrays with the fourth-order difference co-array enhancement, in: 2016 IEEE International Conference on Acoustics, Speech and Signal Processing (ICASSP), 2016, pp. 2991–2995.
- [29] P. Gupta, M. Agrawal, DOA estimation of non-circular signals using fourth order cumulant in underdetermined cases, in: 2018 IEEE International Workshop on Signal Processing Systems (SiPS), 2018, pp. 25–30.
- [30] Svein, Mossige, Algorithms for computing the  $h$ -range of the postage stamp problem, *Math of Computation* 36 (154) (1981) 575–582.
- [31] M. F. Challis, Two new techniques for computing extremal  $h$ -bases  $A_k$ , *The Computer Journal* 36 (2) (1993) 117–126.
- [32] M. F. Challis, J. P. Robinson, Some extremal postage stamp bases, *Journal of Integer Sequences* 13 (2) (2010) 15.
- [33] Z. Fu, P. Charge, Y. Wang, A virtual nested MIMO array exploiting fourth order difference coarray, *IEEE Signal Processing Letters* 27 (2020) 1140–1144.
- [34] J. Steinwandt, F. Roemer, M. Haardt, ESPRIT-type algorithms for a received mixture of circular and strictly non-circular signals, in: 2015 IEEE International Conference on Acoustics, Speech and Signal Processing (ICASSP), 2015, pp. 2809–2813.
- [35] Z. Yang, P. Stoica, J. Tang, Source resolvability of spatial-smoothing-based subspace methods: A hadamard product perspective, *IEEE Transactions on Signal Processing* 67 (10) (2019) 2543–2553.